9

System-Level Simulations Investigating the System-on-Chip Implementation of 60-GHz Transceivers for Wireless Uncompressed HD Video Communications

Domenico Pepe[1] and Domenico Zito[1,2]
[1]*Tyndall National Institute*
[2]*Dept. of Electrical and Electronic Engineering, University College Cork, Cork, Ireland*

1. Introduction

In 2001, the Federal Communications Commission (FCC) allocated an unlicensed 7-GHz wide band in the radio-frequency (RF) spectrum from 57 to 64 GHz for wireless communications (FCC, 2001). This is the widest portion of radio-frequency spectrum ever allocated in an exclusive way for wireless unlicensed applications, allowing multi-gigabit-per-second wireless communications. Other countries worldwide have allocated the 60-GHz band for unlicensed wireless communications (Japan (Ministry of Internal Affairs and Communications [MIC]), 2008), Australia (Australian Communications and Media Authority [ACMA], 2005), Korea (Ministry of Information Communication of Korea, 2006), Europe (ETSI, 2006)), allowing in principle a universal compatibility for the systems operating in that band. Fig. 1 shows the 60-GHz frequency band allocations in USA, Canada, Japan, Australia, Korea and Europe.
Another reason that makes the 60-GHz band very attractive is the coverage range, which is limited to about 10m caused by the dramatic attenuation in the signal propagation. This is due primarily to the high path loss at 60GHz, and moreover the peak of resonance of the oxygen molecule, allowing several Wireless Personal Area Networks (WPANs) to operate closely without interfering. Moreover, at the millimetre-waves (mm-waves) it is easier to implement very directional antennas, thus allowing the implementations of highly directional communication links. Line-Of-Sight (LOS) communication may help in alleviating the design challenges of the wireless transceiver.
One of the most promising applications that will benefit of the huge amount of bandwidth available in the 60-GHz range is the uncompressed High-Definition (HD) video communication (Singh, et al., 2008). The reasons that make attractive the uncompressed video streaming are that compression and decompression (codec) in transmitter and receiver, respectively, exhibit some drawbacks such as latency which can not be tolerated in real time applications (e.g. videogames), degradation in the video quality, and compatibility issues between devices that use different codec techniques. The HD video signal has a resolution of

1920×1080 pixels, with each pixel described by three colour components of 8 bits (24 bits per pixel) and a frame rate of 60Hz. Thus, a data rate of about 3 Gb/s is required for the transmission of the sole video data, without considering audio data and control signals.

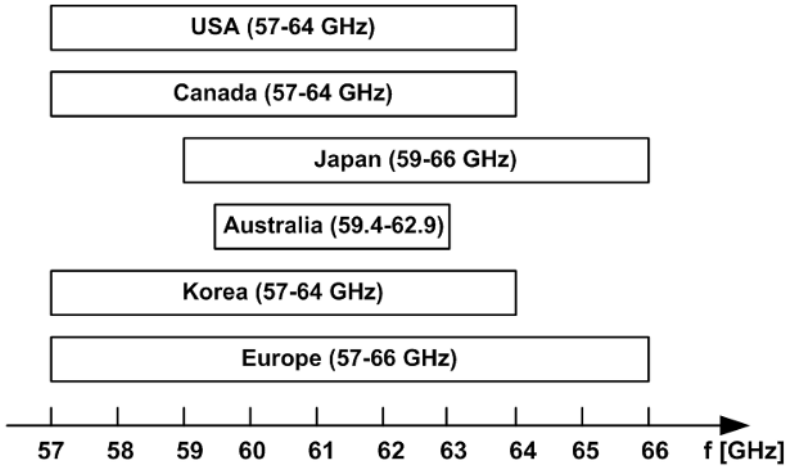

Fig. 1. Worldwide allocations of 60-GHz unlicensed bands

Even though III-V technologies such as Gallium Arsenide (GaAs) allow the implementation of faster active devices, Complementary Metal-Oxide-Semiconductor (CMOS) technology is the best choice for low cost and high volume market applications. The recent advances in silicon technologies allow us to implement integrated transceivers operating at the millimetre-waves, enabling the realization of a new class of mass-market devices for very high data rate communications (Niknejad, 2007). Some 60-GHz building blocks and entire transceivers have been already published (Terry Yao, et al., 2006; Marcu, et al., 2009). In spite of these encouraging results in the integration, there is a lack of the literature on system-level study, which could allow us to get an insight into the implications of the building-blocks specifications and technology potential and limitations about the overall wireless system-on-chip implementation. Such a study could contribute to fulfil this lack of the literature and identify more in detail the circuit- and system-level design challenges, as dealt preliminarly in (Pepe&Zito, 2010a; Pepe&Zito, 2010b).

This Chapter reports a system-level study of a 60-GHz wireless system for uncompressed HD video communications, carried out by means of MATLAB®. In particular, the study is addressed to explore the implementation of 60-GHz transceivers in nano-scale CMOS technology. The implementation in MATLAB® of a model of the high data rate physical layer based on the specification released by the consortium WirelessHD® (WirelessHD, 2009) will be discussed. The system simulations of the bit error rate (BER) are carried out in order to derive the requirements of the 60-GHz transceiver building blocks. This study takes into consideration the performance achievable by using a 65nm CMOS technology. This study includes also system simulations which consider some primary non-idealities of RF transceivers, as the Power Amplifier (PA) non-linearity, Local Oscillator (LO) Phase Noise (PN) and receiver Noise Figure (NF). In Section 2, the standard WirelessHD® is described in short. In Section 3, the system simulations of the High data Rate Physical

layer (HRP) of the 60-GHz system for uncompressed HD video communications by using MATLAB® are described and some results are reported. Moreover, the specifications of the building-blocks are derived. In Section 4, the results of system simulations obtained by taking into account transceiver non-idealities are shown. In Section 5, the conclusions are drawn.

2. Introduction to WirelessHD® specifications

Several international standard organizations and associations of industrial partners are working to define the specifications for millimetre-wave systems operating in the 60-GHz band (IEEE 802.15.3c, 2009; Wireless Gigabit Alliance; WirelessHD). The WirelessHD consortium is an industry-led effort aimed at defining a worldwide standard specification for the next-generation wireless digital network interfaces for consumer electronics and personal computing products. The WirelessHD specifications have been planned and optimized for wireless display connectivity, achieving in its first generation implementation high-speed rates up to 4Gb/s at 10 meters for the consumer electronics, based on the 60-GHz millimetre-wave frequency band. A summary of the specifications required for the High data Rate Physical (HRP) layer is shown in Table 1 (WirelessHD, 2009).
WirelessHD® defines a wireless protocol that enables consumer devices to create a Wireless Video Area Network (WVAN) with the possibility of streaming uncompressed HD video data, at a typical maximum range of 10m. WVANs consist of one Coordinator and zero or more Stations (see Fig. 2). Typically the Coordinator is the sink of the video stream transmitted by the Stations, for example a video display, while the Station can be a source and/or sink of data. The Coordinator and the Stations communicate through a HRP, while the Stations can communicate between each other by means of a Low data Rate Physical layer (LRP). The HRP supports multi-Gb/s throughput at distance of 10m through adaptive antenna technology. The HRP is very directional and can only be used for unidirectional casting. The LRP supports lower data rates and has a omni-directional coverage. A summary of the specifications defined for the HRP layer are shown in Table 1 (WirelessHD, 2009).

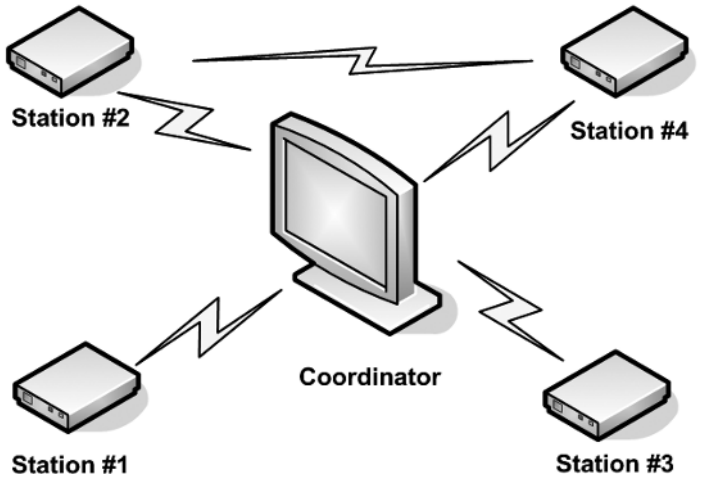

Fig. 2. Scheme of a possible WVAN

Parameter	Value
Bandwidth	1.76 GHz
Reference sampling rate	2.538 GS/s
Number of subcarriers	512
Guard interval	64/ Reference sampling rate
Symbol duration	FFT period+Guard interval
Number of data subcarriers	336
Number of DC subcarriers	3
Number of pilots	16
Number of null subcarriers	157
Modulation	QPSK,16QAM-OFDM
Outer block code	RS(216/224)
Inner code	1/3,2/3(EEP), 4/5+4/7(UEP)
Operating range	10m
BER	$<4x10^{-11}$

Table 1. Summary of the 60-GHz WirelessHD® HRP Specifications

The 57-66GHz band has been divided in four channels for the HRP, of which not all are available everywhere, i.e. depending on the regulatory restrictions of the different countries. A BER of 4×10^{-11} (quasi error-free) at an operating range of 10m is required in order to have a pixel error ratio less than 10^{-9} for 24 bit color. This is achieved by using a concatenated channel code made by an outer Reed-Solomon (216/224) block code and an inner convolutional code, (4/5) and (4/7) for the least significant bits and the most significant bits respectively (Unequal Error Protection, UEP). This is due to the fact that in video communication, unlike data communication, the bits are not equally important: the most significant bits have more impact on the video quality (Singh, et al. 2008), thus the most significant bits are coded with a more robust code.

3. High data rate layer system simulations by MATLAB®

For integrated circuits characterized by a low or moderate complexity, the traditional design approach is bottom-up. Here, the building blocks are designed individually and then co-integrated and verified all together. This approach, while still useful for small systems, exhibits several drawbacks if applied also to large designs. In fact, large designs could require very long simulation time and considerable hardware (since the system is described at transistor level). Moreover, in large designs, the greatest impact on performance and functionality is found at the architectural level more than at the circuit level. Therefore, to address the design of modern integrated circuits characterized by complex architectures and consisting of mixed analog and digital subsystems, a top-down design approach is needed to overcome the limitations of the bottom-up design strategy (Kundert, 2003). In a top-down approach, the architecture is defined by means of block diagrams, so that it could be simulated and optimized by using a system simulator such as MATLAB®. From these system-level simulations, the specifications of the single blocks can be derived accurately. The circuits are designed individually to meet such specifications, and finally the circuits are co-integrated into a single chip. Last, the chip performance are verified and compared with the original requirements.

In Subsection 3.1 the HRP layer based on the 60-GHz WirelessHD communication standard and its modelling in MATLAB® are described. In Subsection 3.2, the results of BER simulations of such system are shown and the specifications of the building blocks for the RF transceiver at 60-GHz are derived.

3.1 HRP transceiver in MATLAB®: description and implementation

In order to evaluate the feasibility and the performance required by the 60-GHz wireless transceivers, system simulations of a high data rate physical layer can be carried out within MATLAB®. The block diagram of the 60-GHz physical layer implemented in MATLAB® is shown in Fig. 3.

After that the uncompressed HD video source data have been processed by the Media Access Control (MAC) layer, an error protection is added to them. The input stream is coded by means of a concatenated channel code made by an outer code (216/224, Reed-Solomon) and an inner code (4/5, 4/7 convolutional). This error protection scheme is fairly robust: in case of Digital Video Broadcasting-Satellite (DVB-S) standard systems described a block diagram similar to that shown in Fig. 3, it can provide a quasi-error free BER of 10^{-10} - 10^{-11} with non-corrected error rates of 10^{-2} (DVB-S; Fisher, 2008). Interleavers are added in order to protect the transmission against burst errors. MATLAB® provides built-in functions for error-control coding and interleaving. Reed-Solomon codes are based on the principle of linear algebra and they protect a block of data with an error protection.

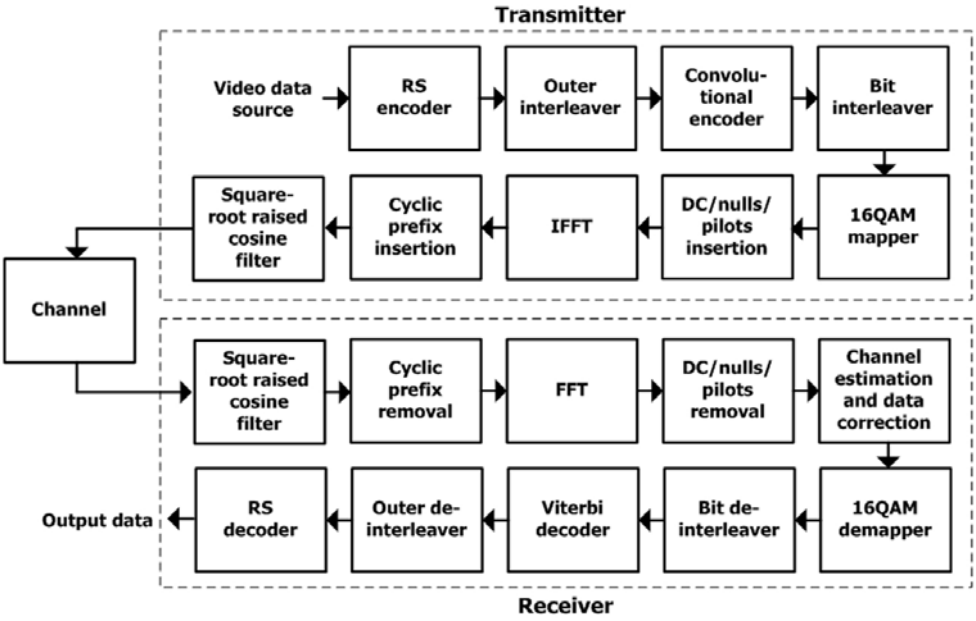

Fig. 3. Block diagram of the 60-GHz WirelessHD HRP model implemented in MATLAB

Reed-Solomon encoder and decoder can be created with the functions `rsenc` and `rsdec` respectively:

```
% RS encoder
RScode=rsenc(msg, nRS, kRS);
...
% RS decoder
decoded = rsdec(rxcode,nRS,kRS);
```

where `msg` is the input string of symbols to be encoded, `nRS` and `kRS` are the length of the encoded and original symbols, 224 and 216, respectively. Interleaving and de-interleaving are easily performed by means of the functions `randintrlv` and `randdeintrlv`.
The convolutional encoder uses a constrain length equal to 7, mother code rate 1/3, generator polynomial g0=133oct, g1=171oct, g2= 165oct (IEEE, 2009). The standard require eight parallel convolutional encoders, in which the first four encoders for the first outer Reed-Solomon coding branch and the last four encoders for the second outer Reed-Solomon coding branch. In Equal Error Protection (EEP) mode all the eight encoders shall use the same inner code rate. In the UEP mode, the top four encoders shall use rate 4/7 convolutional codes, while the bottom four encoders shall use rate 4/5 convolutional codes. In order to ease the simulations, the EEP mode has been considered, with a punctured code rate of 2/3 (obtained by the mother code 1/3). Convolutional encoded data is punctured in order to make the desired code rate using the puncturing pattern [1 1 1 0 0 0]. The code implemented in MATLAB® is shown hereinafter.

```
% Convolutional encoding
trellis=poly2trellis(7,[133 171 165]);
punctcode=convenc(outerbits, trellis, [1 1 1 0 0 0]);
…
% Convolutional decoding
decodedmsg=vitdec(rxmsg, trellis, tblen, 'trunc', 'hard',
[1 1 1 0 0 0]);
```

`poly2trellis` is a function that converts the convolutional code polynomials to a trellis description. That is used by the function `convenc, that` encodes the binary vector `outerbits` using the convolutional encoder whose MATLAB trellis structure is `trellis`, applying the punctured pattern [1 1 1 0 0 0]. On the decoder side, the function `vitdec` decodes the vector `rxmsg` using the Viterbi algorithm.
After the coding operation, the data are modulated. A data rate of 3.807Gb/s is achieved by employing a 16 Quadrature Amplitude Modulation (QAM) - Orthogonal Frequency-Division Multiplexing (OFDM) modulation (WirelessHD, 2009). The bits are grouped in

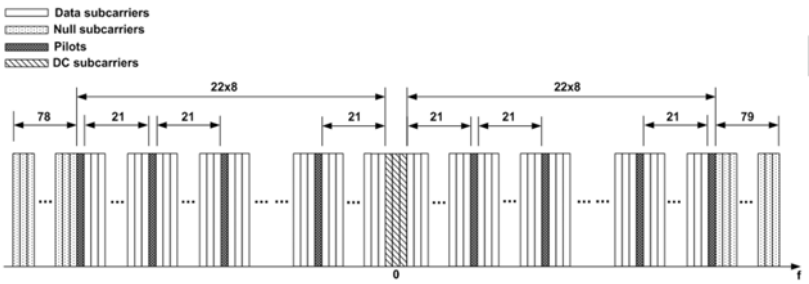

Fig. 4. OFDM symbol in the frequency domain (with the specific choice of pilots, dc and nulls subcarriers)

symbols of four bits each, having values between 0 and 2^4-1=15. These data are sent to the symbol mapper, which maps the input bits into 16QAM Gray-coded symbols. The 16QAM mapper and demapper can be implemented by means of the functions `qammod` and `qamdemod` available in MATLAB®. The output data of the symbol mapper are then parallelized, and pilots, dc and null tones are added up. The pilot tones are used for frame detection, carrier frequency offset estimation and channel estimation (Chiu, et al., 2000). Typically the central subcarriers are not used since they correspond to a dc component in baseband. The outer subcarriers are usually unused for data transmission in order to allow a low-pass filtering with a larger transition band after the digital to analog converter (Olsson & Johansonn, 2005). The HRP subcarriers in a OFDM symbols could be allocated as shown in Fig. 4.
An Inverse Fast Fourier Transform (IFFT) operation (size 512) is then applied to the resulting stream in order to have OFDM symbols in which each subcarrier is modulated by the 16QAM symbols provided by the mapper, dc, nulls and pilots. In order to improve the immunity to inter-symbol interferences, a cyclic prefix consisting of the last 64 samples of the symbol is inserted at the beginning of the OFDM symbol itself. A section of code of the modulator and cyclic prefix insertion is reported hereinafter.

```
% 16QAM modulation
16qammod=qammod(4bitsymbols, 16, 0, 'gray');
modreshaped=reshape(16qammod, 336, mappedmsglenght/336).';
% dc, nulls, pilots insertion
ofdmsymbolf=[zeros(mappedmsglenght/336,78)
   pilot*ones(mappedmsglenght/336,1)
         modreshaped(:,[1:21]) ...
…
% OFDM modulation
 ofdmsymbolt=ifft(ofdmsymbolf.').';
% cyclix prefix insertion
 ofdmsymbolt=[ofdmsymbolt (:,[449:512]) ofdmsymbolt];
```

The data stream is shaped by means of a square-root raised cosine filter and then transmitted.
As for the receiver, after that the down-conversion and filtering have been performed, the cyclic prefix is removed from the OFDM symbol, and the Fast Fourier Transform (FFT) operation is carried out on the received stream. Since the output of the de-mapper is sensitive to the amplitude of the input symbols, a block for channel estimation and gain correction has been implemented in MATLAB®. For each OFDM symbol received, the channel response C(k) is estimated extracting the amplitude received pilot values and dividing them by the expected values as follows:

$$C(k)=\frac{P_{RX}(k)}{P(k)} \tag{1}$$

where k is the pilot index, $P_{RX}(k)$ are the amplitude of received pilot values and P(k) the amplitude of the expected pilots. Then the data subcarriers are multiplied by the inverse of the coefficient C(k) of the nearest pilot tone.
System simulations have been performed by considering an Additive White Gaussian Noise (AWGN) channel. The BER simulations of the system shown in Fig. 3 have been carried out. In particular, an input string of about 6,000,000 bits has been used as source for the 60-GHz

system, limited by the hardware capabilities of our workstation. The curves of the BER at the input of the baseband receiver, before and after the concatenated channel coded blocks, are shown in Fig. 5.

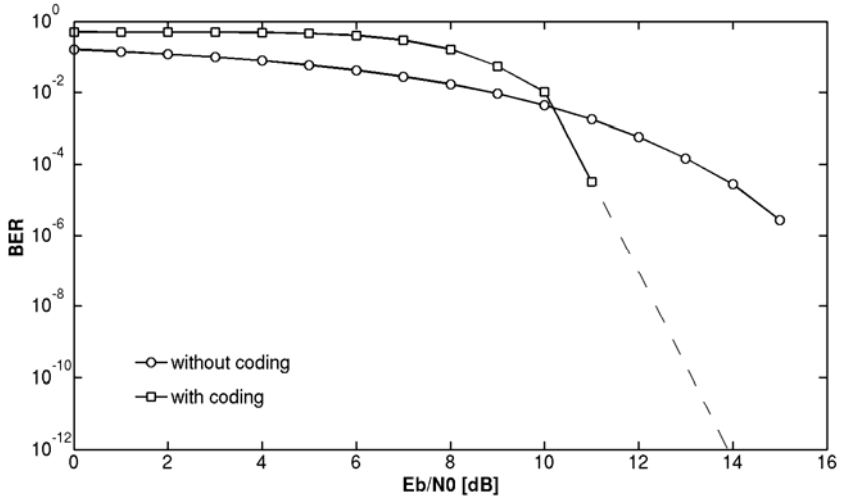

Fig. 5. BER with and without concatenated channel coding. The dashed line is a linear extrapolation of the BER curve obtained by means of simulations of the system of Fig. 3

By extending linearly the last part of the curve of the BER (that is a worsening condition with respect to the real case), we obtain a BER of 4×10^{-11} for a energy per bit to noise power spectral density ratio (Eb/N0) lower than 14 dB, which corresponds to a signal-to-noise ratio (SNR) of 16.74 dB, as calculated from the formula

$$\begin{aligned}\left.\mathrm{SNR}\right|_{\mathrm{dB}} = \left.\mathrm{Eb/N0}\right|_{\mathrm{dB}} &+10\times\mathrm{Log}_{10}k+10\times\mathrm{Log}_{10}\left(\frac{\mathrm{dsc}}{\mathrm{nFFT}}\right)+10\times\mathrm{Log}_{10}\left(\frac{\mathrm{nFFT}}{\mathrm{nFFT+CP}}\right)+\\ &+10\times\mathrm{Log}_{10}\left(\frac{\mathrm{kRS}}{\mathrm{nRS}}\right)+10\times\mathrm{Log}_{10}\left(\frac{\mathrm{kCon}}{\mathrm{nCon}}\right)\end{aligned} \tag{2}$$

where $k=\mathrm{Log}_2(M)$ and M is the size of the modulation (16 in this case), dsc is the number of data subcarriers (336), nFFT the FFT size (512), CP is the guard interval (64), kRS/nRS is the Reed-Solomon coding rate (216/224) and kCon/nCon is the convolutional coding rate (2/3).

3.2 HRP transceiver in MATLAB®: simulation results and system specifications

From the system simulations described in Section 3 we can see that a SNR of 16.74 dB allows the achievement of a quasi-error free BER of 4×10^{-11}. A SNR of 23 dB has been considered to have 6 dB of margin at least. The receiver sensitivity is equal to

$$\left.S_{RX}\right|_{\mathrm{dB}} = \left.k_B T\right|_{\mathrm{dB}} +10\times\mathrm{Log}_{10}(B)+\left.\mathrm{SNR}\right|_{\mathrm{dB}} +\left.\mathrm{NF}\right|_{\mathrm{dB}} \tag{3}$$

where k_B is the Boltzmann constant (1.23×10^{-23}[W/K]), T is the antenna temperature (290K), B the occupied bandwidth (2GHz) and NF the receiver noise figure. In order to have a

receiver sensitivity of at least -50 dBm (Karaoguz, 2009), NF is required to be lower than 8 dB. This value is achievable in latest CMOS processes, e.g. 65nm.
In this study, we consider direct-conversion transceivers (homodyne, see Fig. 6) since in principle they allow the highest level of integration.

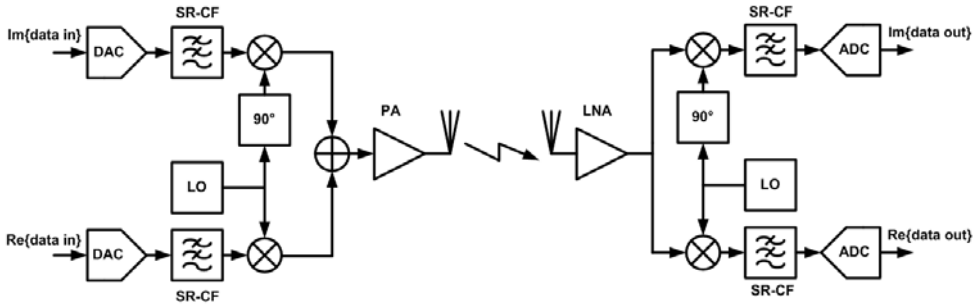

Fig. 6. Block diagram of a homodyne transceiver

Therefore, by taking into account the capabilities of the 65nm CMOS technology at 60 GHz, if we consider the achievable performance for a Low Noise Amplifier (LNA) such as a gain of 15 dB and noise figure of 6 dB (Terry Yao, et al., 2007; Huang, et al., 2009; Zito, et al., 2007)) and for the mixer, such as a gain of -2dB and noise figure of 15 dB (Zhang, et al., 2009)), the resulting noise figure of the LNA-Mixer cascade equals to 6.5 dB.
At 60 GHz the path loss is very high. At 10m (this is the operating range required by the standard WirelessHD®) the free-space path loss amounts to

$$PL\Big|_{dB} = \left(\frac{4\pi df}{c}\right)^2\Bigg|_{dB} = 88dB \tag{4}$$

where d is the operating range (10m), f is the carrier frequency (60 GHz) and c is the speed of light in air (3×10^8).
Thus, it results that the power delivered by the power amplifier has to be quite high in order to provide a signal with adequate power at the receiver antenna. The typical antenna gain is expected to be 10 to 20 dBi (Karaoguz, 2009). If we consider an antenna gain of 10 dB (both in transmission and reception) and NF of 7 dB, then the output power delivered by the PA has to be 14 dBm, at least, in order to achieve an operating range of 10m. This is a high value for the CMOS implementation of the PA. Recently, examples of PAs with 1-dB compression point higher than 14 dBm have been reported in literature (Law, et al., 2010; Jen, et al., 2009). In spite of this, the PA has to be also highly linear, since OFDM modulation is characterized by a very high peak-to-average power ratio (the back-off amounts approximately to 10dB).

4. Transceiver non-idealities

The performance of radio-frequency transceivers are usually described by means of deterministic quantities such as gain, noise, linearity, bandwidth. On the other hand, digital baseband circuitry performance are described in terms of statistic quantities, such as the BER. In order to fill the gap between digital and RF circuits, models running in both the

environments are needed. Radio-frequency behavioural models allow us to introduce radio-frequency non-linearity and simulate their effects in the overall system comprehensive of the digital baseband part (Kundert, 2003; Chen, 2006). Behavioural models of the building blocks of the RF transceiver can be developed within MATLAB® and inserted into the overall system model description in order to evaluate how the transceiver non-linearities affect the performance of the system.

4.1 Power amplifier non-linearity effects

Since OFDM modulation presents a very high peak-to-average power ratio, the effect of PA non-linearity can not be neglected in system simulations.
The output voltage (v_{out}) of a memory-less non-linear amplifier can be expressed by:

$$v_{out}(t)=a_1 v_{in}(t)+a_2 v_{in}^2(t)+a_3 v_{in}^3(t)+... \tag{5}$$

where v_{in} is the input voltage.
By applying a sinusoidal input voltage at frequency ω_0 ($v_{in} = V_0\cos(\omega_0 t)$) the output can be expressed as follows:

$$v_{out}(t)=\frac{a_2 V_0^2}{2}+\left(a_1 V_0+\frac{3a_3 V_0^3}{4}\right)\cos(\omega_0 t)+\frac{a_2 V_0^2}{2}\cos(2\omega_0 t)+\frac{a_3 V_0^3}{4}\cos(3\omega_0 t)+... \tag{6}$$

If we consider the fundamental harmonic only, the Input-referred 1-dB Compression Point (ICP1dB) can be calculated from the formula

$$20\log(a_1 V_{i1dB})\text{-}1dB=20\log\left(a_1 v_i+\frac{3}{4}a_3 v_i^3\right) \tag{7}$$

where V_{i1dB} is the voltage ICP1dB.
The third-order polynomial model above of the PA can be implemented in MATLAB® in order to include the non-linear effects of the gain compression of power amplifier in system simulations. By exploiting Equation (7), the MATLAB® code of the PA can be written as follows:

```
PA_ICP1dB_dBm=PA_OCP1dB_dBm-PA_gain_dB+1;
PA_IV1dB_dB=PA_ICP1dB_dBm-30; % dBm to dB
PA_IV1dB=10.^(PA_IV1dB_dB/20) % dB to linear
PA_Vgain=10.^(PA_gain_dB/20);
PAout=ofdmsymbolt.*PA_Vgain-
          (ofdmsymbolt.^3).*(0.11.*PA_Vgain.*(1/(PA_IV1dB.^2)));
```

where `PA_gain_dB` and `PA_Vgain` are the PA gain (dB and linear voltage gain) set to obtain the desired average transmitted output power (i.e., 15 dBm in this study), and `PA_OCP1dB_dBm` is the Output-referred 1-dB Compression Point (OCP1dB) of the PA. The input-output characteristic of a PA, with 15-dB gain and 20-dBm OCP1dB, is shown in Fig. 7.
Fig. 8 reports the results of BER simulations for an average transmitted power of 15 dBm for several values of OCP1dB. Note that BER performance are practically unaffected for OCP1dB 10dB higher than the average transmitted power. The BER is still acceptable for OCP1dB 5dB higher than the average transmitted power, whereas for an OCP1dB equal to the average transmitted power the BER is impaired significantly.

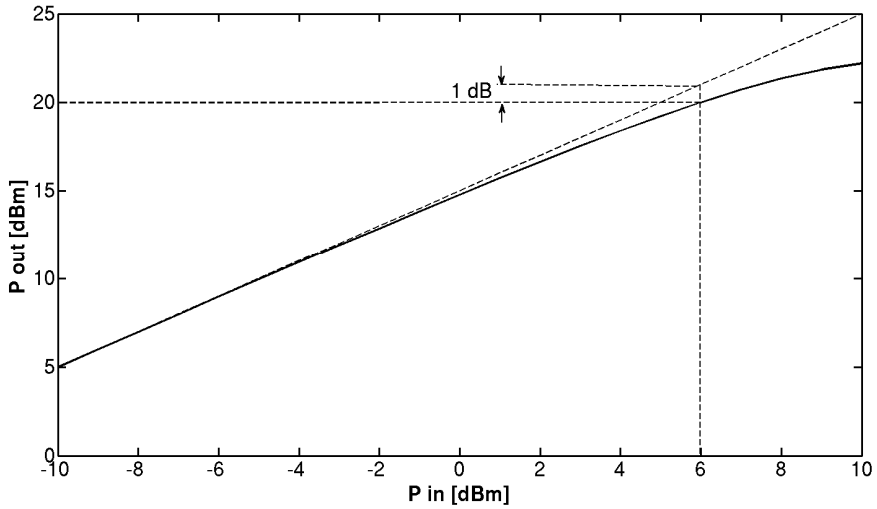

Fig. 7. Input-output characteristic of a power amplifier

These system simulations have been carried out by simulating the overall system comprehensive of the Forward Error Correction (FEC) blocks (i.e., Reed-Solomon and convolutional coding). In order to make faster simulations, BER system simulations without FEC can be performed, and then the coding gain can be applied later (i.e. from simulation results shown in Fig. we can see that for Eb/N0=14dB the BER drops from $\approx 5*10^{-4}$ without FEC to $\approx 10^{-12}$ with FEC).

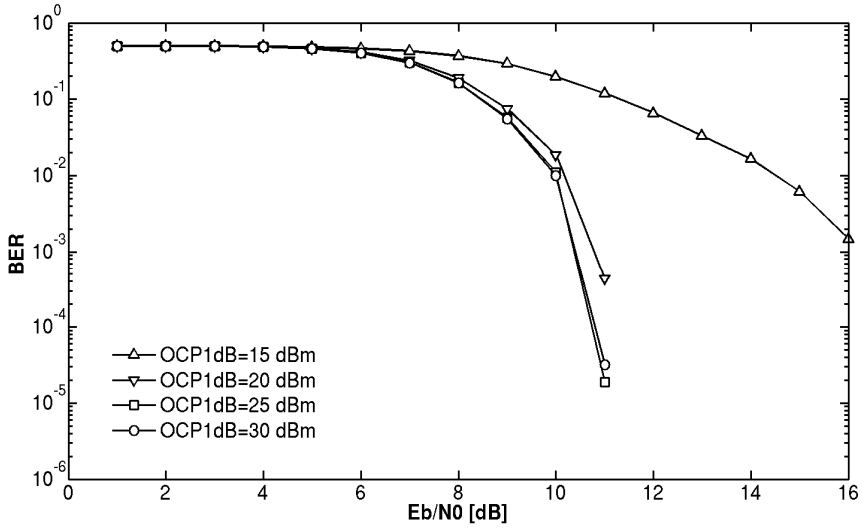

Fig. 8. BER versus Eb/N0 for several values of the output referred 1-dB compression point of the power amplifier, for an average transmitted power of of 15 dBm

4.2 Local oscillator phase noise effects

A simple model of the local oscillator phase noise can be implemented in MATLAB® in order to investigate how the phase noise affects the performance of the entire system. In order to do that, a time domain phase noise generator model has to be implemented. In this case study the Power Spectral Density (PSD) of the phase noise is modelled with a Lorentzian shape. The Lorentzian spectrum is constant at low frequencies and rolls off with a first order slope after the corner frequency (Chen, 2006). The phase noise is generated by filtering a White Gaussian Noise (WGN) through a digital filter. The power of the WGN (P_{WGN}) can be expressed as follows:

$$P_{WGN}[dB]=P_{PHASE}\big|_{dB}+PN\big|_{dB}+10\times\log(f_s)+10\times\log\left(\frac{1MHz}{f_p}\right) \quad (8)$$

where P_{PHASE} is equal to π^2, PN is the Phase Noise, f_s is the sampling frequency and f_p the corner frequency of the Lorentzian spectrum. This noise is by a first order low pass digital filter with corner frequency equal to f_p (MATLAB® code reported hereinafter).

```
% white gaussian noise
noise=wgn(m, n, Pwgn,'dBW');
% filtering
b=[1 1];
a=[(1+fs/(pi*fp)) (1-fs/(pi*fp))];
pnoise=filter(b,a,noise_wgn);
```

The normalized PSD of the LO voltage noise for f_s=100MHz and f_p=10kHz is shown in Fig. 9.

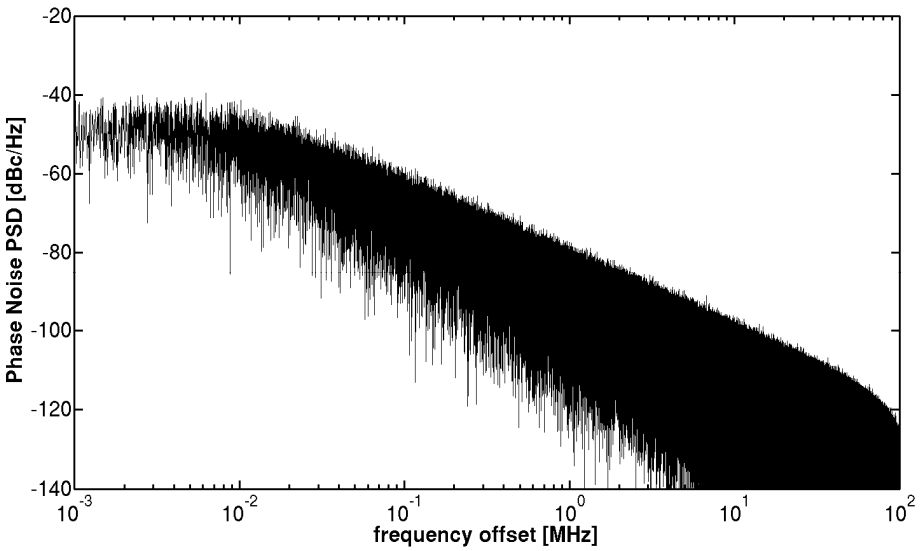

Fig. 9. PSD of the phase noise modeled in MATLAB®

In the system simulations the phase noise has been added to both the LOs of the transmitter and receiver. The BER performance for several value of LO phase noise are shown in Fig. 10. It can be noted how this system is very sensitive to the phase noise and that acceptable results are obtained only for PN lower than -100dBc/Hz.

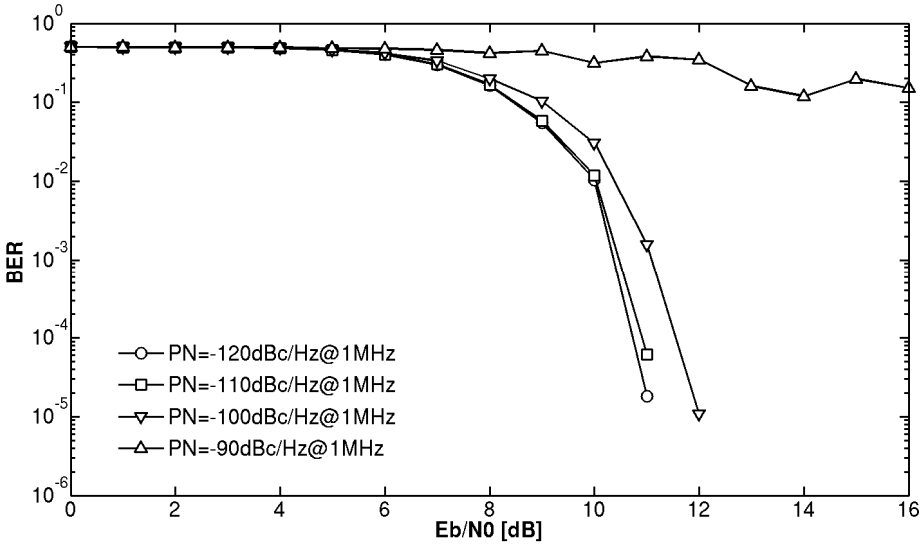

Fig. 10. BER versus Eb/N0 for several values of PN

4.3 System simulations by taking into account transceivers non-idealities

System simulations have been carried out considering an average transmitted power of 15 dBm, PA OCP1dB equal to 20 dBm, LO phase noise equal to -100dBc/Hz and noise figure of the receiver chain (i.e. LNA and mixer) equal to 7 dB, for AWGN and fading channels (Rician and Rayleigh). The results in terms of BER versus transmitter-receiver distance are shown in Fig. 11.

Acceptable performance are obtained also in case of fading channels. This is due to the channel coding, the adaptive filter at the receiver and the modulation scheme (OFDM) that is fairly robust in presence of fading channels.

It is worth mentioning that the specifications calculated in Subsection 4.1 are related to a transceiver with single-transmitter and single-receiver. In practice, the overall transceiver could be implemented on silicon by exploiting multiple transceivers connected to an array of highly directional antennas (Gilbert, et al., 2008; Doan, et al., 2004). This way, not only the antenna beam-form can be steered in order to improve the link between transmitter and receiver, but also the specifications of transmitters and receivers will be more relaxed, since the power delivered will be N times greater than that delivered by a unit element and the receiver noise figure will be reduced of $10\times\text{Log}_{10}\text{N}$ dB, where N is the number of transceivers in parallel.

Note that an increase in the number of elements of the array leads to higher power consumption of the overall communication system, thus a trade-off between performance and power consumption has to be taken into account for the optimal design of the wireless transceiver.

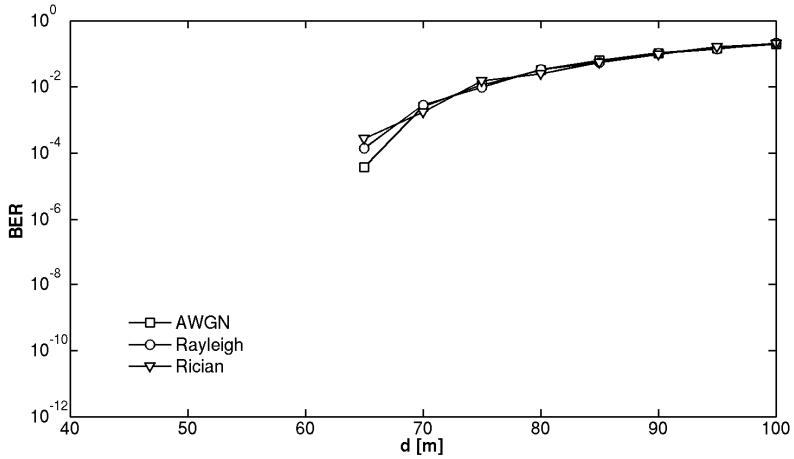

Fig. 11. BER versus distance for AWGN, Rayleigh and Rician channels

5. Conclusion

In 2001, the FCC allocated an unlicensed 7-GHz band in the 60GHz radio frequency range for wireless communications. This band is the widest portion of radio-frequency spectrum ever allocated for wireless applications, allowing multi-gigabit-per-second wireless communications. One of the most promising applications, that will benefit of such a huge amount of bandwidth, is the uncompressed HD video streaming. In this Chapter, a 60-GHz system for the emerging wireless uncompressed video communication has been studied and the possibility of realizing transceivers integrated in CMOS technology has been investigated. To address the design of modern integrated circuits, that can have complex architectures and made by mixed analog and digital subsystems as this one, a top-down design approach is needed. The architecture of the chip can be defined as a block diagram, and simulated and optimized using MATLAB® as a system simulator. A model of the high data rate physical layer, based on the specifications released by the consortium WirelessHD®, has been implemented in MATLAB® and system simulations have been carried out. These simulations allowed us to investigate the feasibility of the wireless transceiver in CMOS technology and to derive the preliminary specifications of its building blocks for a System-on-Chip implementation. The impact of transceiver non-idealities, such as PA non-linearity, LO phase noise, LNA and mixer noise on the BER have been investigated through system simulations made within MATLAB®. This study confirms the opportunity offered by MATLAB® as system-level CAD tool for the design, simulation and optimization of very complex system-on-chip, including analog, mixed-signals and digital integrated circuits, such as CMOS 60-GHz transceivers for emerging high-speed wireless applications.

6. Acknowledgment

This work has been supported in part by Science Foundation Ireland (SFI) under Grant 08/IN.1/I854 and Irish Research Council for Science, Engineering and Technology (IRCSET) under Grant R13485.

7. References

Australian Communications and Media Authority, (2005), Radiocommunications (Low Interference Potential Devices) Class License Variation 2005 (no. 1)

Chen, J.E. (May 2006). Modeling RF Systems, Available from http://www.designers-guide.org/Modeling/modeling-rf-systems.pdf

Chiu, Y. ; Markovic, D.; Tang, H. ; Zhang, N. (December 2000). OFDM receiver design, Final Report 12/12/2000, University of California Berkeley

Doan, C.H. ; Emami, S. ; Sobel, D.A. ; Niknejad, A.M. ; Brodersen, R.W. (2004). Design considerations for 60 GHz CMOS radios, *IEEE Communication Magazine*, Vol. 42, No. 12, (December 2004), pp. 132-140, ISSN 0163-6804

DVB-S Standard in a nut shell, Available from http://www.complextoreal.com/dvbs.htm

ETSI DTR/ERM-RM-049, (2006). Electromagnetic compatibility and Radio spectrum Matters (ERM); System Reference Document; Technical Characteristics of Multiple Gigabit Wireless Systems in the 60 GHz Range

Federal Communications Commission, (2001). Code of Federal Regulation, title 47 Telecommunication, Chapter 1, part 15.255

Fisher, W. (2008). *Digital Video and Audio Broadcasting Technology: A Practical Engineering Guide*, Springer, ISBN 978-3-540-76358-1, Germany

Gilbert, J.M. ; Doan, C. H. ; Emami, S. ; Shung, C.B. (2008). A 4-Gbps Uncompressed Wireless HD A/V Transceiver Chipset, *IEEE Micro*, Vol. 28, No. 2, (March-April 2008), pp. 56-64, ISSN 0272-1732

Huang, B.-J. ; Lin, K.-Y. ; Wang, H. (2009), Millimeter-Wave Low Power and Miniature CMOS Multicascode Low-Noise Amplifiers with Noise Reduction Topology, *IEEE Transactions on Microwave Theory and Techniques*, Vol. 52, No. 12, (December 2009), pp. 3049-3059, ISSN 0018-9480

IEEE, (October 2009). Part 15.3: Wireless Medium Access Control (MAC) and Physical Layer (PHY) Specifications for High Rate Wireless Personal Area Networks (WPANs)

IEEE 802.15 WPAN Task Group 3c (TG3c) Millimeter Wave Alternative PHY, Available from http://ieee802.org/15/pub/TG3c.html

Jen, Y.-N. ; Tsai, J.–H. ; Huang, T.-W. ; Wang, H. (2009). Design and analysis of a 55-71 GHz compact and broadband distributed active transformer power amplifier in 90-nm CMOS process, *IEEE Transaction on Microwave Techinques and Theory*, Vol. 57, No. 7, (July 2009), pp. 1637-1646, ISSN 0018-9480

Karaoguz J., (September 2009). IEEE 802.11-09-0960-00-00ad, Wireless HD Specification and Coexistance Capabilities, Available from: https://mentor.ieee.org/802.11/dcn/09/11-09-0960-00-00ad-wirelesshd-coexistence.ppt

Kundert, K. (February 2003). Principles of Top-Down Mixed-Signal Design, Available from http://www.designers-guide.org/Design/tdd-principles.pdf

Law, C.Y. & Pham, A.-V. (2010). A high-gain 60GHz power amplifier with 20dBm output power in 90nm CMOS, *Digest of Technical Papers of IEEE International Solid-State Circuits Conference*, pp. 426–427, ISSN 0193-6530, San Francisco, California, USA, February 7-11, 2010

Marcu, C.; Chowdhury, D.; Thakkar, C.; Jung-Dong Park; Ling-Kai Kong; Tabesh, M.; Yanjie Wang; Afshar, B.; Gupta, A.; Arbabian, A.; Gambini, S.; Zamani, R.; Alon, E.;

Niknejad, A.M. (2009). A 90 nm CMOS low-power 60GHz transceiver with integrated baseband circuitry, *IEEE Journal of Solid-State Circuits,* Vol.44 , No.12, (December 2009), pp. 3434-3447, ISSN 0018-9200

Ministry of Information Communication of Korea, (2006). Frequency Allocation Comment of 60 GHz band

Ministry of Internal Affairs and Communications, (2008). Frequency Assignment Plan, Available from: http://www.tele.soumu.go.jp/e/adm/freq/search/share/plan.htm

Niknejad, A. (2007). 0-60 GHz in Four Years: 60 GHz RF in Digital CMOS, *IEEE Solid-State Circuits Newsletter*, Vol.12, No.2, (Spring 2007), pp. 5-9, ISSN 1098-4232

Ollson, M. & Johansson, H. (2005). OFDM Carrier Frequency Offset Estimation Using Null Subcarriers, *10th International OFDM Workshop*, Hamburg, Germany, August 30-September 1, 2005

Pepe, D. & Zito, D. (2010a). 60-GHz CMOS Transceivers for Uncompressed Wireless HD Video Communication, *Proceedings of the Royal Irish Academy Committee for Communications and Radio Science, Research Colloquium on Wireless as an Enabling Technology: Innovation for a Critical infrastructure*, pp. 115-117, ISBN:978-1-904890-3, Dublin, Ireland, April 21-22, 2010

Pepe, D. & Zito, D. (2010b). 60-GHz transceivers for wireless HD uncompressed video communication in nano-era CMOS technology, *Proceedings of 15th IEEE Mediterranean Electrotechnical Conference*, pp. 1237 – 1240, ISBN 978-1-4244-5793-9, La Valletta, Malta, April 26-28, 2010

Singh, H.; Jisung, O. ; Changyeul, K. ; Xiangping, Q. ; Huai-Rong, S. ; Chiu, N. (2008). A 60 GHz wireless network for enabling uncompressed video communication, *IEEE Communications Magazine,* Vol.46, No.12, (December 2008), pp. 71-78, ISSN 0163-6804

Terry Yao; Gordon M. Q.; Tang K.K.W.; Yau K.H.K.; Ming-Ta Yang; Schvan P.; Voinigescu S. P. (2007). Algorithmic Design of CMOS LNAs and PAs for 60-GHz Radio, *IEEE Journal of Solid-State Circuits*, Vol. 42, No. 5, (May 2007), pp. 1044–1057, ISSN 0018-9200

Wireless Gigabit Alliance, Available from http://wirelessgigabitalliance.org/

WirelessHD, Available from http://www.wirelesshd.org/

WirelessHD (August 2009). WirelessHD Specification Overview, Available from http://www.wirelesshd.org/pdfs/WirelessHD-Specification-Overview-v1%200%204%20Aug09.pdf

Zhang, N. ; Xu, H. ; Wu, H.-T. ; O, K.K. (2009). W-Band Active Down-Conversion Mixer in Bulk CMOS, *IEEE Microwave and Wireless Components Letters*, Vol. 19, No. 2, (February 2009), pp. 98-100, ISSN 0018-9200

Zito, D.; Pepe, D.; Neri, B.; Taris, T.; Begueret, J.-B.; Deval, Y.; Belot, D. (2007). A Novel LNA Topology with Transformer-based Input Integrated Matching and its 60-GHz Millimeter-wave CMOS 65-nm Design, *Proceedings of IEEE International Conference on Electronics, Circuits and Systems*, pp. 1340-1343, ISBN 978-1-4244-1377-5, Marrakesh, Morocco, December 11-14, 2007

Applications of MATLAB in Science and Engineering

Edited by Prof. Tadeusz Michalowski

ISBN 978-953-307-708-6
Hard cover, 510 pages
Publisher InTech
Published online 09, September, 2011
Published in print edition September, 2011

The book consists of 24 chapters illustrating a wide range of areas where MATLAB tools are applied. These areas include mathematics, physics, chemistry and chemical engineering, mechanical engineering, biological (molecular biology) and medical sciences, communication and control systems, digital signal, image and video processing, system modeling and simulation. Many interesting problems have been included throughout the book, and its contents will be beneficial for students and professionals in wide areas of interest.

How to reference

In order to correctly reference this scholarly work, feel free to copy and paste the following:

Domenico Pepe and Domenico Zito (2011). System-Level Simulations Investigating the System-on-Chip Implementation of 60-GHz Transceivers for Wireless Uncompressed HD Video Communications, Applications of MATLAB in Science and Engineering, Prof. Tadeusz Michalowski (Ed.), ISBN: 978-953-307-708-6, InTech, Available from: http://www.intechopen.com/books/applications-of-matlab-in-science-and-engineering/system-level-simulations-investigating-the-system-on-chip-implementation-of-60-ghz-transceivers-for-

INTECH
open science | open minds

InTech Europe
University Campus STeP Ri
Slavka Krautzeka 83/A
51000 Rijeka, Croatia
Phone: +385 (51) 770 447
Fax: +385 (51) 686 166
www.intechopen.com

InTech China
Unit 405, Office Block, Hotel Equatorial Shanghai
No.65, Yan An Road (West), Shanghai, 200040, China
中国上海市延安西路65号上海国际贵都大饭店办公楼405单元
Phone: +86-21-62489820
Fax: +86-21-62489821